3048–3056 *Nucleic Acids Research, 2005, Vol. 33, No. 9*
doi:10.1093/nar/gki608

Global analysis of yeast RNA processing identifies new targets of RNase III and uncovers a link between tRNA 5′ end processing and tRNA splicing

Shawna L. Hiley[1], Tomas Babak[1,2] and Timothy R. Hughes[1,2,*]

[1]Banting and Best Department of Medical Research, University of Toronto, 112 College Street, Toronto, ON M5G 1L6, Canada and [2]Department of Medical Genetics and Microbiology, University of Toronto, 1 King's College Circle, Toronto, ON M5S 1A8, Canada

Received April 1, 2005; Revised and Accepted May 3, 2005

ABSTRACT

We used a microarray containing probes that tile all known yeast noncoding RNAs (ncRNAs) to investigate RNA biogenesis on a global scale. The microarray verified a general loss of Box C/D snoRNAs in the TetO_7-*BCD1* mutant, which had previously been shown for only a handful of snoRNAs. We also monitored the accumulation of improperly processed flank sequences of pre-RNAs in strains depleted for known RNA nucleases, including RNase III, Dbr1p, Xrn1p, Rat1p and components of the exosome and RNase P complexes. Among the hundreds of aberrant RNA processing events detected, two novel substrates of Rnt1p (the RUF1 and RUF3 snoRNAs) were identified. We also identified a relationship between tRNA 5′ end processing and tRNA splicing, processes that were previously thought to be independent. This analysis demonstrates the applicability of microarray technology to the study of global analysis of ncRNA synthesis and provides an extensive directory of processing events mediated by yeast ncRNA processing enzymes.

INTRODUCTION

Noncoding RNA (ncRNA), which includes nuclear and mitochondrial rRNA and tRNA, snRNA, snoRNA, and the RNA components RNase P and MRP, telomerase and the signal recognition particle, accounts for 95% of the total nucleic acid in cells (1) and shows a high level of functional conservation across species. Many ncRNAs undergo extensive post-transcriptional processing in the form of exo- and endonucleolytic cleavage of precursor transcripts [e.g. (2,3)] and covalent modification (4,5). Although most of the major nucleases in yeast are known, these enzymes target multiple substrates and the complete set of targets is not well understood (3). Moreover, the relationships between processing events are also incompletely understood. For example, little is known about the relative order of tRNA processing events, although they presumably occur sequentially because the various tRNA processing and modifying enzymes have diverse subcellular localizations (6,7).

Standard methods for characterizing RNA processing events include primer extension and northern blotting, neither of which is amenable to high-throughput analysis. Microarrays designed to measure yeast ncRNAs have previously been used to characterize RNA processing events (8–10). For example, we recently designed a tiling microarray to cover all known and several predicted yeast ncRNAs at ~5 nt intervals (11,12). However, in these previous studies the microarray probe sequences were short; in our design this was intentional, in order to maximize the detection of differences in binding affinity of modified and unmodified RNAs on the microarray. As a consequence, low-abundance transcripts and regions of RNAs with highly stable secondary structures were detected with reduced efficiency (11).

In the present study, we applied this microarray strategy to the problem of general RNA biogenesis and processing, particularly the cleavage of precursor RNAs to their mature functional form. We first designed and tested a microarray with longer oligonucleotide target sequences to enable more uniform detection of transcripts of varied abundance. In order to allow the study of processing events, the microarray includes oligonucleotide probes that tile 100 nt of flanking sequence on both the 5′ and 3′ ends of each ncRNA transcript. We then analyzed mutants in the major yeast ncRNA processing nucleases. Two novel targets of Rnt1p and a novel link between tRNA 5′ end processing and tRNA splicing were identified. This work provides new insights into the target sites and specific roles of the yeast ncRNA processing machinery, as well as an extensive database of ncRNA processing events that will

*To whom correspondence should be addressed. Tel: +1 416 946 8260; Fax: +1 416 978 8528; Email: t.hughes@utoronto.ca

facilitate a more comprehensive understanding of yeast RNA biogenesis.

MATERIALS AND METHODS

Microarray design and construction

Oligonucleotide sequences are contained in the Supplementary Material. Oligonucleotides were designed to be complementary to known ncRNA sequences and flanking regions and were tiled at 5 nt intervals for most RNAs (intron-containing mRNAs were tiled every 20 nt and mitochondrial RNAs every 15 nt). Probe lengths were adjusted to have a melting temperature of ~53°C. Ink-jet microarrays were manufactured by Agilent Technologies (Palo Alto, CA).

Strains

Homozygous deletion mutants (13) were obtained from Research Genetics. $TetO_7$-promoter alleles were constructed as described previously (14). *rnt1-1*^{ts} (15) and corresponding wild-type control strain W303-1a were kindly provided by Sherif Abou Elela; *rat1-1*^{ts} (16) and corresponding control strain FY23 were provided by Steve Buratowski. Strain numbers are as follows: $TetO_7$-*BCD1*: TH_3235; *dbr1-Δ*: TH_138; *rat1-1*^{ts}: TH_7097; $TetO_7$-*RNT1*: TH_3029; *rnt1-1*^{ts}: TH_6855; $TetO_7$-*RRP46*: TH_2706; $TetO_7$-*MTR3*: TH_3685; *rrp6-Δ*: TH_387; $TetO_7$-*POP1*: TH_2654; $TetO_7$-*POP4*: TH_5545; *xrn1-Δ*: TH_3339. The wild-type control for tet-promoter strains was R1158 (14); for deletion strains, BY4743 (13).

RNA isolation and microarray analysis

Isogenic wild-type and mutant strains were grown in parallel at 30°C in SC medium (with the exception of the temperature-sensitive alleles; see below) with shaking in baffled flasks (Bellco) to final cell concentrations matched as closely as possible to 10^7cells/ml. $TetO_7$-promoter strains were exposed to 10 μg/ml doxycycline for a total of 20–24 h. Temperature-sensitive strains were grown at 23°C overnight, then shifted to 37°C for 4 h. For conditional mutants, the doubling times in Table 2 are based on growth under restrictive conditions. The cells were harvested and RNA extracted as described previously (10). Ten micrograms of DNase I-treated RNA was labeled with Alexa Fluor 546 or 647 according to the manufacturer's instructions (Molecular Probes 'Ulysis' kit), ethanol-precipitated and hybridized to the microarray as described previously (17). Formamide was added to a final concentration of 33%, as described previously (17). Hybridizations were carried out in a rotating incubator at 42°C for 18 h and washed as described previously (17). Microarrays were scanned on an Axon 4000B instrument.

Image processing, microarray data normalization and data visualization

Scanned images were quantified with GenePix 3.0 (Axon Instruments). Individual channels were spatially detrended (i.e. overall correlations between spot intensity and position on the slide removed) and normalized as described previously (11), resulting in $\log_2$ intensities and ratios of mutant versus wild type.

Data availability

Microarray oligonucleotide sequences and microarray data are found at http://hugheslab.med.utoronto.ca/Hiley_nuc. Spreadsheets containing the data displayed in Figure 2 are also available on the website.

Northern blots

For northern blot analysis, 5 μg of total RNA from each strain (isolated and treated with DNase I as described above) was separated on 10% denaturing polyacrylamide–urea gels and transferred to a Hybond-XL membrane (Amersham) in 0.5× TBE using a semi-dry transfer apparatus (Bio-Rad). Membranes were UV-crosslinked and hybridized in Church buffer using 5′-^{32}P-end-labeled complementary oligonucleotide probes as indicated in the figures. Images were visualized using a PhosphorImager (Bio-Rad Personal FX). Probe sequences were as follows (5′ to 3′): (Figure 3B) RUF3 5′flank, CACACGTACTAGACTTTATCTGTCTTGATTG; RUF3 body, CAATTGTTGTAGTCGCAACTACGGTAATTG; RUF1 5′ flank, GTACTCTCATTAACTAGCTCTGTTATTC; RUF1 body, AAAAAGTCGCAACCTCAATCATGCCTTTTCTC; (Figure 4C) tRNA LeuCAA 5′ flank, GGCCAAACAACCACTTATTTGTATGTTTCG; tRNA LeuCAA intron, TATTCCCACAGTTAACTGCGGTCAAGATATTG; tRNA LeuCAA exon 1, CTTGAATCAGGCGCCTTAGACCGCTC.

RESULTS

Longer oligonucleotide probes improve the detection of RNAs

To increase the sensitivity of detection of directly labeled RNA transcripts, we created a version of our previously described microarray (11) with longer oligonucleotide probes (see Supplementary Material for probe sequences). This new microarray features probes tiled across the same ncRNA sequences, but has an average probe length of 25.1 nt [compared with 18.4 nt on the previous microarray (11)]. A comparison of the two microarrays using wild-type RNA revealed that the longer probes improved the consistency and detection levels of both tRNAs (Figure 1A) and rRNA (Figure 1B). Furthermore, we were able to detect a greater proportion of less abundant RNA transcripts (e.g. snoRNAs, Figure 1C). Although microarray spot intensity is a relative measurement (controlled by the photomultiplier tube voltage on the scanner), the fact that the flanking sequences (representing background) are slightly darker (i.e. there is lower signal-to-noise) in all of the short-oligonucleotide plots in Figure 1 confirms that the overall signal-to-noise ratio is superior on the long-oligonucleotide microarray.

General loss of Box C/D snoRNAs in a $TetO_7$-*BCD1* strain

To further validate the new microarray, we analyzed RNA from a strain with the *BCD1* ('Box C/D snoRNAs') gene under the control of the tetracycline-responsive promoter ($TetO_7$-*BCD1*). We previously demonstrated that *BCD1* is required for biogenesis and/or stability of Box C/D snoRNAs (10). However, the previous classification was based on the reduction of only 11 Box C/D snoRNAs, but not 2 box H/ACA

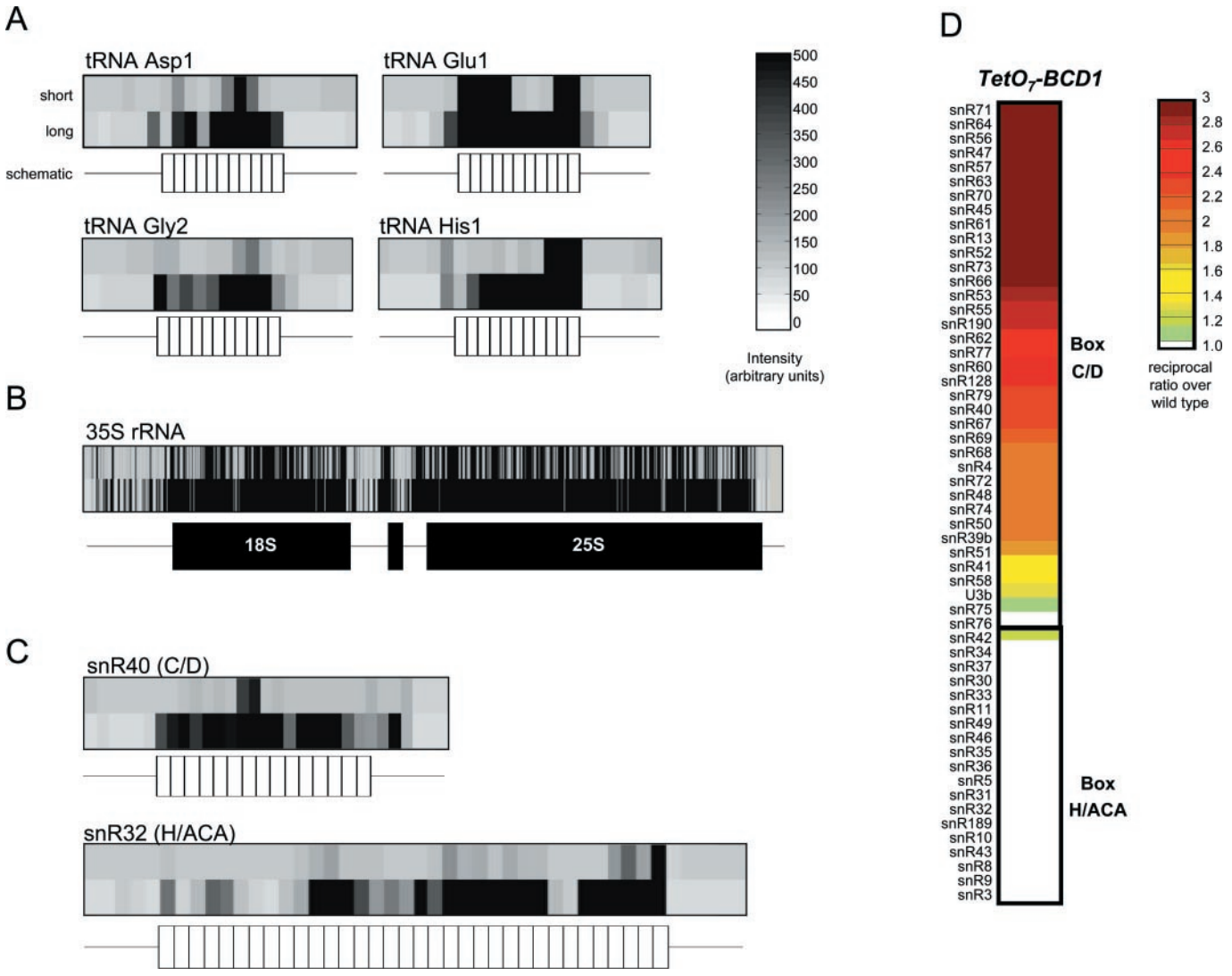

Figure 1. Longer oligonucleotide probes improve the sensitivity of detection. The intensity of fluorescence of wild-type RNA bound to probes on either short (top) or long (bottom) oligonucleotide microarrays, shaded according to the color bar on the right, is plotted for representative transcripts: (**A**) tRNAs, (**B**) 35S pre-rRNA and (**C**) snoRNAs. Schematic diagrams of the RNAs and flanking regions are shown below with boxes representing RNA sequence and thin lines indicating flanking sequence. (**D**) Box C/D RNA depletion in a TetO$_7$-*BCD1* strain. The relative fluorescence of Box C/D and Box H/ACA snoRNA probes is shown, colored according to the scale on the right. Note that because the reciprocal of the mutant:wild-type ratio is plotted in this panel, increasing red color indicates depletion of snoRNAs.

snoRNAs, in the TetO$_7$-*BCD1* strain. In order to investigate the role of this protein on a more comprehensive scale, we analyzed TetO$_7$-*BCD1* RNA on the new microarray, which encompasses all 84 known snoRNAs. In this experiment, RNA isolated from wild-type cells (labeled with Cy3) and RNA isolated from mutant yeast cells (labeled with Cy5) were hybridized to the microarray simultaneously, and the fluorescence in each channel was measured and compared as a ratio [(mutant RNA fluorescence)/(wild-type RNA fluorescence)] (see Materials and Methods for details). We observed the depletion of virtually all Box C/D snoRNAs, but there was essentially no effect on Box H/ACA snoRNAs (Figure 1D). This confirms the widespread involvement of Bcd1p in Box C/D snoRNA and/or snoRNP biogenesis, and also verifies that the majority of snoRNA probes are detecting the correct signal, since they specifically register a reduction in the amount of the RNA they are designed to detect.

Microarray detection of nucleolytic RNA processing events

We next analyzed strains deficient in nucleases known to be required for the processing of rRNA, tRNA, snoRNA, snRNA and mRNA introns (Table 1; growth rates of mutant strains are contained in Table 2). We expected that flanking sequences that are improperly processed in mutant strains would accumulate and result in a positive ratio, as previously seen using a smaller microarray (10).

To gain an initial overview of the results, we used clustering analysis to examine the data from oligonucleotide probes with ratios >4/1 (mutant/wild type) and corresponding to flanking regions (Figure 2, left hand side). Probes corresponding to accumulated flanking regions are colored according to the color bar shown, and the identities of the probes are indicated in the monochrome schematic on the right of Figure 2. It is

Table 1. Yeast RNA nucleases and their principal known RNA targets

Nuclease	Type	Complex	Principal known ncRNA targets
RRP46	3′–5′ exonuclease	Exosome	35S 5′–A_0, ITS2 E-C_2, snRNA and snoRNA 3′ ends
MTR3	3′–5′ exonuclease	Exosome	35S 5′–A_0, ITS2 E-C_2, snRNA and snoRNA 3′ ends
RRP6	3′–5′ exonuclease	Exosome	35S 5′–A_0, ITS2 E-C_2, snRNA and snoRNA 3′ ends
POP1	Endonuclease	RNaseP/MRP	tRNA 5′ leader, 35S ITS1 A_3–B_1
POP4	Endonuclease	RNaseP/MRP	tRNA 5′ leader, 35S ITS1 A_3–B_1
RNT1	Endonuclease	N/A	35S 3′ ETS, snRNAs and snoRNA 5′ends
RAT1	5′–3′ exonuclease	N/A	35S A_0–A_1, A_2–A_3, 3′ ETS
XRN1	5′–3′ exonuclease	N/A	35S A_0–A_1, D–A_2, A_2–A_3

Table 2. Growth rates of mutant strains

Strain	Doubling time (h)
dbr1-Δ	1.4
rat1-1^{ts}	3.4
TetO$_7$-*RNT1*	11.5
rnt1-1^{ts}	2.1
TetO$_7$-*RRP46*	5.4
TetO$_7$-*MTR3*	9.9
rrp6-Δ	2.0
TetO$_7$-*POP1*	4.9
TetO$_7$-*POP4*	2.7
xrn1-Δ	3.6
TetO$_7$-*BCD1*	3.5

evident that the majority of probes corresponding to any given type of processed fragment behave similarly (i.e. cluster together) and accumulate in mutants known to be responsible for their processing. The specificity of detection of the expected events is demonstrated by the relatively small number of apparent false-positive probes (i.e. probes that accumulate in mutants that are not thought to have a role in their processing) clustering in the unexpected regions of the figure (i.e. outside the black regions in the right hand panel). For example, Dbr1p is the enzyme responsible for debranching the lariat intron generated by mRNA splicing, a step that is necessary for the degradation of intronic RNA by the cell (18). Figure 2 shows that there is a specific accumulation of mRNA introns in the *dbr1-Δ* strain. We did not observe an accumulation of tRNA introns (Supplementary Material), consistent with the fact that splicing of tRNAs proceeds through the tRNA splicing endonuclease (SEN) complex rather than the spliceosome (19). However, we did observe the accumulation of intron-encoded snoRNAs, consistent with previous analysis (20). This experiment showed an impressive level of specificity, with 195 of the 200 highest ratio probes corresponding to intron sequences processed by the spliceosome (Supplementary Material; the other five probes in the top 200 correspond to unrelated tRNA and rRNA sequences, likely representing noise in the data).

In some cases, flanking regions are processed by more than one enzyme. For example, the rRNA 3′ external transcribed sequence (ETS) is cleaved from the primary transcript by Rnt1p and is then degraded by Rat1p (3). This is detected in our data: both temperature-sensitive and tetracycline-regulated alleles of *RNT1*, as well as a *rat1-1^{ts}* mutant, accumulated 3′ ETS sequences in this analysis. A similar phenomenon is seen for the 5′ ETS: deletion of *RAT1* impaired processing of 5′ ETS sequences A_0–A_1 in the 5′ ETS and A_2–A_3 in internal transcribed sequence 1 (ITS1), while deletion of *XRN1* resulted in the accumulation of both A_0–A_1 sequences as well as ITS1 sequences D–A_2 and A_2–A_3.

These data also underscore differences in phenotypes of mutants in proteins that have similar functions. Rrp46p and Mtr3p are both core components of the exosome, while Rrp6p is specific to the nuclear exosome. Mutations in all three enzymes resulted in the accumulation of sequences between the 5′ end of the transcript and A_0 in the 5′ ETS, as well as in the second ITS2 between E and C2. However, depletion of Rrp46p and Mtr3p primarily impact 35S pre-rRNA processing, while the rrp6 mutant largely accumulates snoRNA 3′ flank sequences, consistent with prior observations (3,21).

These data are posted in their entirety at http://hugheslab.med.utoronto.ca/Hiley_nuc and are available as a Supplemental Data file accessible via the journal's website. While the data primarily reflect known roles of these RNA processing enzymes, there are numerous examples of processing events that to our knowledge have not been previously characterized. Two selected instances of particular interest that we have confirmed by directed analysis are described here.

Additional targets of Rnt1p

We observed novel processing events involving Rnt1p (RNase III), an endonuclease with many known targets in yeast, including rRNA, snRNAs and snoRNAs [reviewed in (3)]. We analyzed RNA from two strains containing different mutant alleles of *RNT1* by microarray (TetO$_7$-*RNT1* and *rnt1-1^{ts}*; Figures 2 and 3A; Supplementary Material). In addition to the accumulation of known targets (e.g. 35S 3′ ETS and Box C/D snoRNA 5′ flank sequences), we observed the accumulation of 5′ flank sequences of both RUF1 and RUF3 RNAs (Figure 3A). Initially identified as ncRNA transcripts by a comparative genomic strategy, these RNAs of Unknown Function were classified as Box H/ACA snoRNAs (22,23). To confirm that these snoRNAs are indeed processed by Rnt1p, we performed northern blot analysis of RUF3 RNA isolated from strains depleted for Rnt1p (Figure 3B, top). Strains containing either conditional allele of *RNT1* accumulated an extended RUF3 species in addition to the mature RNA. Reprobing the same blot (after stripping the first probe) with a 5′ leader-specific probe confirmed that the larger RNA in both strains is a 5′-extended version. Identical results were obtained from northern analysis of RUF1 (Figure 3B, bottom). Similar to other Rnt1p targets, the 5′ flank sequences of both RUF1 and RUF3 are predicted to contain a consensus AGNN tetraloop upstream of the cleavage site (Figure 3C) (24,25). Together, these data reconfirm RUF1 and RUF3 as bona fide RNAs and establish that they are processed at the 5′ end by Rnt1p.

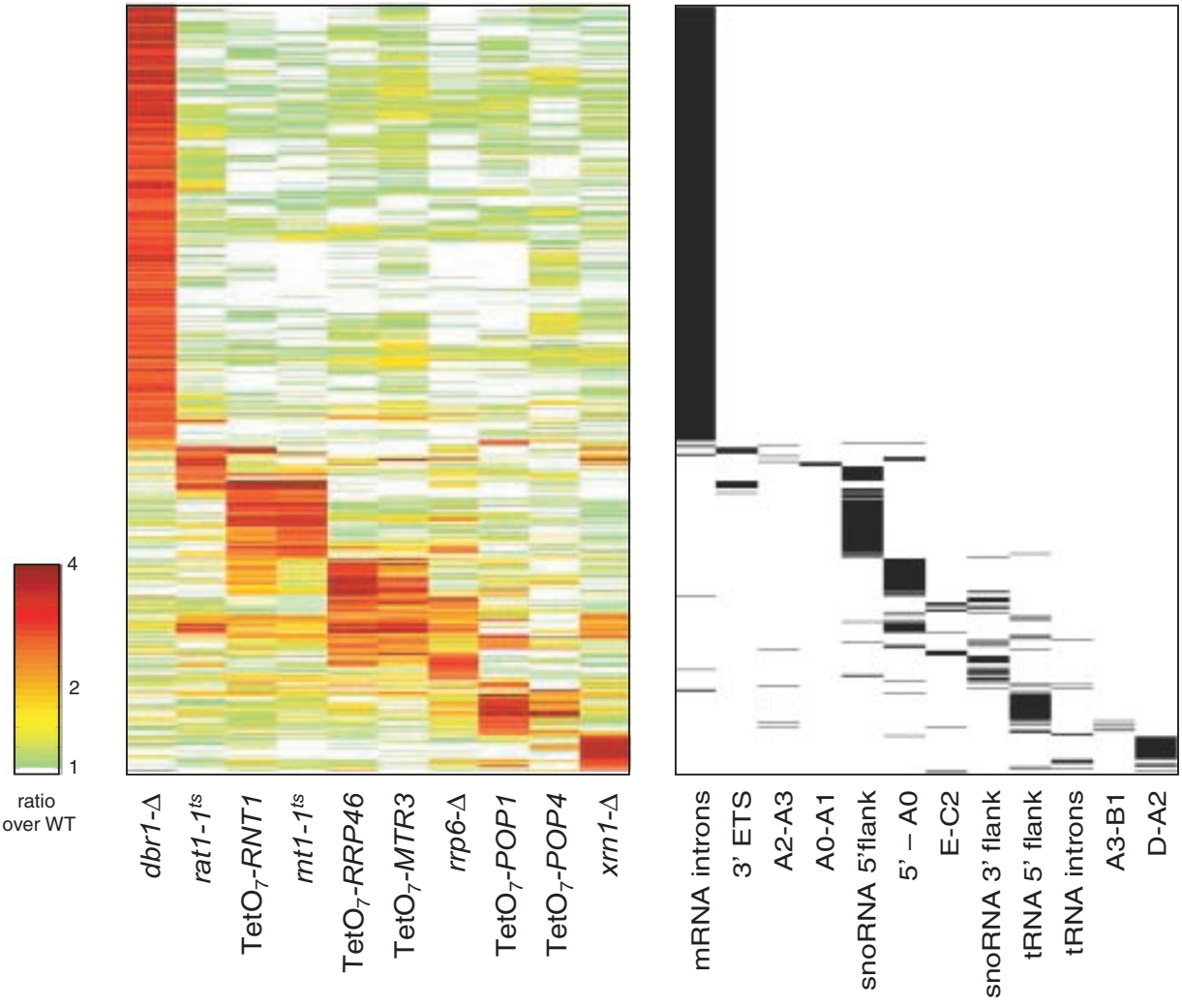

Figure 2. Detecting known RNA processing events by microarray. Oligonucleotides corresponding to processed regions showing at least a 4-fold increase at least one of the mutant strains were subjected to hierarchical agglomerative clustering. Probes corresponding to accumulated sequences are colored red, according to the scale shown. The identities of the probes are shown in the black and white panel on the right. A fully labeled numerical version of this figure is available in the Supplementary Material.

A link between 5′ processing and tRNA splicing

tRNAs in yeast are extensively processed: they are subject to both 5′ and 3′ end processing (6,26), many covalent modifications (5), and intron-containing tRNAs are spliced by the SEN complex (19). Pop1p and Pop4p are protein components of RNase P (the ribonucleoprotein complex responsible for removing the 5′ leader sequence from tRNAs) and RNase MRP (which processes sequences between A3 and B1 in the 35S pre-rRNA transcript). We analyzed RNA from strains with tetracycline-regulated alleles of *POP1* and *POP4* by microarray and observed the accumulation of both tRNA 5′ leader and A3-B1 sequences (Figure 2). Figure 4A shows schematic diagrams of selected tRNAs with the relative fluorescence from the $TetO_7$-*POP1* and $TetO_7$-*POP4* experiments as described above. The concentration of high-ratio (i.e. red) probes in the region immediately 5′ of the mature tRNA (highlighted in red on the schematic) indicates that the leader sequences are accumulating in both mutants.

In addition to the accumulation of 5′ leader sequences, we observed the accumulation of intron sequences in several intron-containing tRNAs (Figure 4A, LeuCAA and LysCTT). This was surprising because it was thought that there is no relationship between tRNA 5′ end processing and tRNA splicing (27). To confirm that this effect was caused by the depletion of the RNase P complex and not a general response to slow growth or depletion of an essential gene product, we compared the relative fluorescence of LeuCAA tRNA probes in nine different experiments (Figure 4B). Accumulation of tRNA intron probes was exclusive to the two experiments affecting the RNase P complex. We next performed northern blot analysis of LeuCAA tRNA from $TetO_7$-*POP1* and $TetO_7$-*POP4* strains. Figure 4C confirms that the $TetO_7$-*POP1* and $TetO_7$-*POP4* strains accumulated unspliced, 5′ leader-containing RNA. These strains also contained a roughly equivalent amount of spliced leader-containing RNA (Figure 4C). As a control, we analyzed RNA from a strain with a tetracycline-regulated allele of *SEN34*, the catalytic subunit

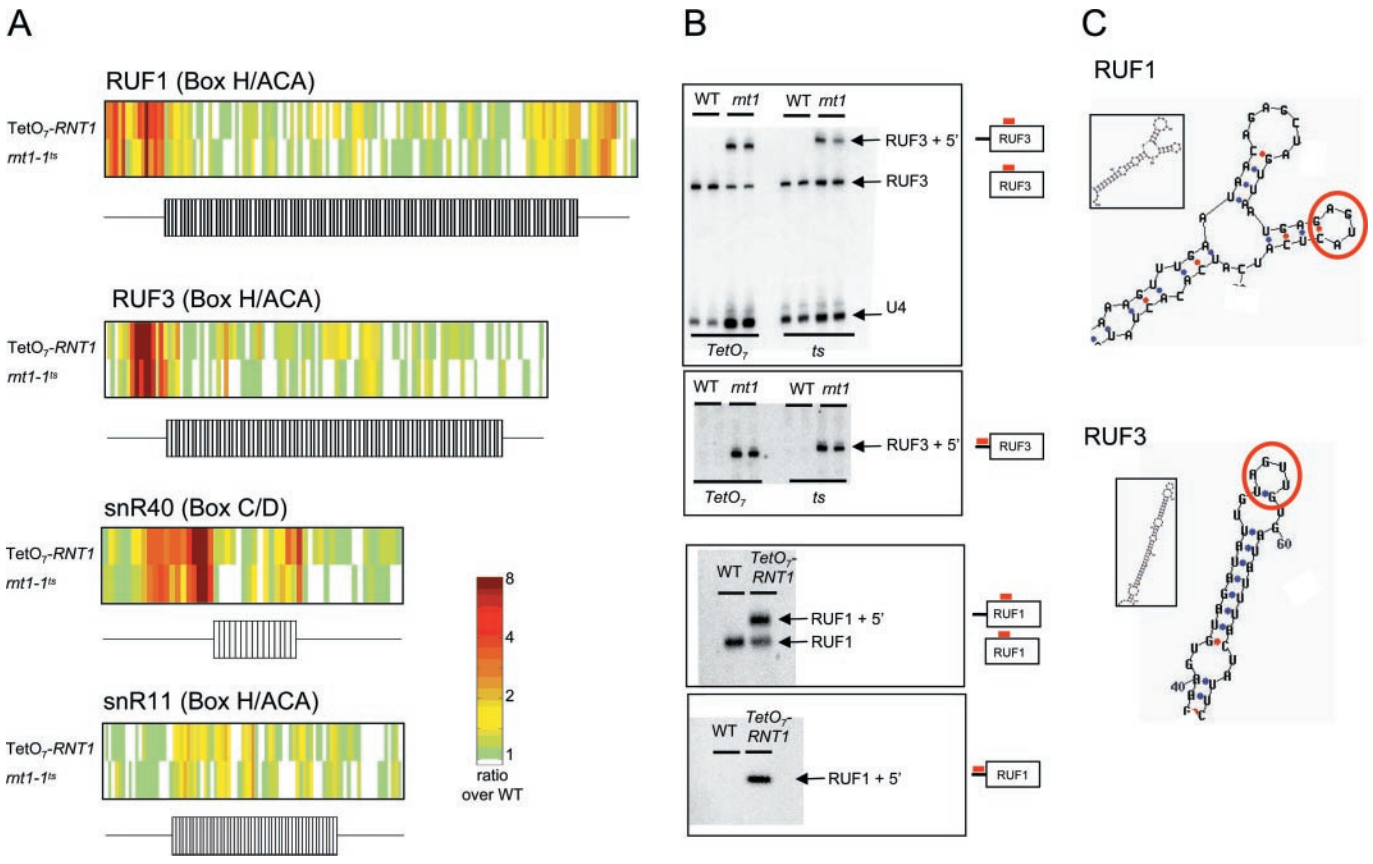

Figure 3. The 5′ ends of RUF1 and RUF3 are processed by Rnt1p. (**A**) Relative fluorescence of probes from analysis of TetO$_7$-*RNT1* and *rnt1-1*^{ts} strains is shown, with schematic diagrams of the RNAs below as described in Figure 1. (**B**) Northern blot analysis of RUF3 and RUF1 RNA in wild-type and Rnt1p-deficient strains. The blots were probed sequentially with two different probes (the positions of which are shown on the schematic diagrams). Two replicates of each sample were loaded side-by-side; U4 RNA was probed as a loading control. (**C**) Predicted structures of 5′ flank sequences of RUF1 and RUF3, based on Mfold structure prediction (25). The inset shows the full predicted structure of the 5′ leader. The AGNN tetraloop in each RNA is circled in red.

of the tRNA SEN. As expected, this strain accumulated the intron-containing (but not 5′ extended) tRNA (Figure 4C, center blot). Together, these data indicate that the presence of the 5′ leader does not prevent, but may delay splicing as ~50% of the 5′ leader-containing RNA is unspliced (compared with <5% of tRNA with a mature 5′ end in the wild-type samples). Conversely, the presence of the intron had no effect on the removal of the 5′ leader, as shown by the complete removal of the leader in the TetO$_7$-*SEN34* experiment. The northern blot in Figure 4C (left) also appears as though it may contain 3′ unprocessed forms, consistent with previous demonstrations that 5′ processing generally precedes 3′ processing (26,28). Because there is no mutant known to be defective specifically in tRNA 3′ end processing, we did not examine further the relative ordering of 5′ and 3′ steps, or the ability of the arrays to measure such a defect.

DISCUSSION

To study RNA biogenesis on a global scale, we developed an improved tiling microarray that monitors the synthesis and processing of all known ncRNAs in *Saccharomyces cerevisiae*. We demonstrated the ability of the microarray to detect a reduction in steady-state levels of snoRNAs in a TetO$_7$-*BCD1* mutant, and to detect perturbation of many known rRNA, snoRNA and tRNA processing events in appropriate nuclease mutants.

In addition to detecting known targets, we identified Box H/ACA snoRNAs RUF1 and RUF3 (22,23) as novel substrates of Rnt1p. Rnt1p cleavage sites require no sequence conservation, but all Rnt1p substrates identified to date contain an AGNN tetraloop 14–17 nt away from the cleavage site (29). The predicted structures of the 5′ leader sequences from both *RUF1* and *RUF3* contain AGNN loop sequences (Figure 3C) in highly structured regions. In contrast to Box C/D snoRNAs, most of which are 5′ processed by Rnt1, previous to this study only three known Box H/ACA snoRNAs were known to share this processing pathway (30); we detected two of these by microarray. Our results show that more H/ACAs are processed at the 5′ end by Rnt1p than were previously appreciated.

In addition, we discovered a previously undescribed relationship between tRNA 5′ processing and tRNA splicing (Figure 4). Our analysis revealed an accumulation of both tRNA introns and 5′ leader sequences in strains depleted for protein components of the RNase P complex (Figure 4B). The fact that ~50% of tRNA in these strains was spliced (and still contained the 5′ leader) suggests that the removal of the leader sequence is not absolutely required in order for splicing to take place, but rather may affect the kinetics of the reaction. The converse, however, is not true: consistent with previous studies

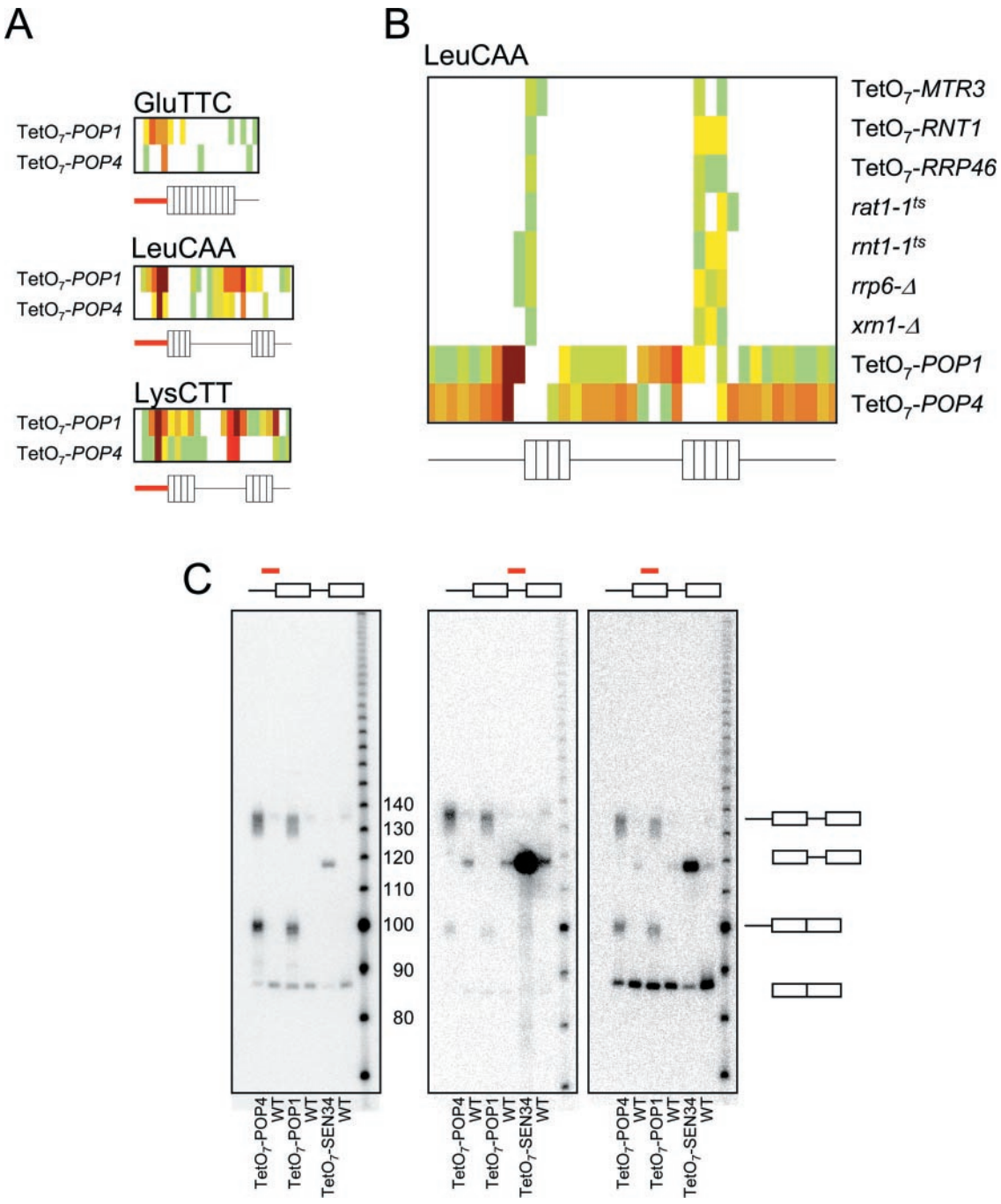

Figure 4. Microarray analysis reveals a partial dependence of tRNA splicing on tRNA 5′ end processing. (**A**) Relative fluorescence of probes complementary to select tRNAs are shown with schematic diagrams below. (**B**) Relative fluorescence of LeuCAA tRNA probes is shown for the nine microarray experiments shown in Figure 2A. (**C**) Northern blot analysis of LeuCAA tRNA species present in TetO$_7$-*POP1* and *POP4* strains is shown. The same blot was probed sequentially with three different probes, as indicated by the schematic diagrams at the top of each blot (with the red line indicating the position of the probe). The identity of each tRNA species is shown to the right.

(31–33), we observed that the presence of tRNA introns does not interfere with the ability of the cell to process flank sequences from the ends of tRNAs (Figure 4B).

On the basis of localization of tRNA genes and tRNA processing enzymes, it is possible to construct a simple model of the sequence of tRNA biogenesis. tRNA genes tend to be clustered in the nucleolus (34). RNase P is also found in the nucleolus (7,35), as are most intron-containing tRNAs (36,37). The SEN complex, however, is localized to the outer mitochondrial membrane (6,7,38). This implies that tRNA 5′ end processing is likely to occur in the nucleolus and thus should precede splicing, which likely occurs in the cytoplasm (38). However, to our knowledge, previous evidence indicates that these processes are independent (27). A previous study of tRNA processing in yeast splicing utilized northern blots with intron-specific probes to detect tRNA

precursors, splicing intermediates and products (27) in wild-type yeast cells. Because intron-containing species with both 5′ leaders and 3′ extensions were detected, it was concluded that the processes of tRNA splicing and intron removal are not ordered with respect to each other (27). Although the authors attempted to measure the relative amounts of various tRNA species, they acknowledged that the measurements made represent steady-state levels, and that processing kinetics was not estimated. Our data suggest that tRNA splicing is at least partially dependent upon tRNA 5′ end processing, which could represent a reduction in either accessibility of 5′ unprocessed tRNAs to the SEN complex (perhaps via reduced transport out of the nucleolus) or a direct inhibition of the splicing reaction. This phenomenon is reminiscent of the inhibition of pre-mRNA splicing by disruption of 5′ end capping (39) and could represent a potential example of functional coupling in pre-tRNA processing. While still a steady-state analysis, the microarray data presented here provide a more complete quantification of the products of tRNA processing because all tRNAs were examined comprehensively.

Genome sequencing and subsequent efforts to characterize the transcriptome and to predict functions for all of the encoded proteins have underscored the importance of ncRNA (10,22,40,41). New techniques are needed to fully characterize the synthesis and processing of ncRNA in many different organisms. The technique described here could be applied by any laboratory to study ncRNA processing in any yeast mutant of interest. Moreover, with the recent availability of siRNA and shRNA constructs to 'knock-down' individual mammalian mRNAs (42,43), it should be possible to recapitulate this type of analysis in vertebrate cells. The analysis we present here demonstrates the utility of microarray technology for the discovery of RNA processing events in a relatively well-studied organisms. We anticipate that it will be fruitful to extend this approach to other organisms.

SUPPLEMENTARY MATERIAL

Supplementary Material is available at NAR Online.

ACKNOWLEDGEMENTS

The authors thank Drs Sherif Abou Elela and Steve Buratowski for providing strains, and Gwenael Badis-Breard, Ben Blencowe and Denis Lafontaine for critical evaluation of the manuscript. This work was supported by CIHR and CFI grants to T.R.H., a CIHR post-doctoral fellowship to S.L.H. and an NSERC graduate scholarship to T.B. Funding to pay the Open Access publication charges for this article was provided by CIHR.

Conflict of interest statement. None declared.

REFERENCES

1. Sherman,F. (2002) Getting started with yeast. *Methods Enzymol.*, **350**, 3–41.
2. Allmang,C., Kufel,J., Chanfreau,G., Mitchell,P., Petfalski,E. and Tollervey,D. (1999) Functions of the exosome in rRNA, snoRNA and snRNA synthesis. *Embo J.*, **18**, 5399–5410.
3. Venema,J. and Tollervey,D. (1999) *Ribosome synthesis in Saccharomyces cerevisiae*. *Annu. Rev. Genet.*, **33**, 261–311.
4. Decatur,W.A. and Fournier,M.J. (2002) rRNA modifications and ribosome function. *Trends Biochem. Sci.*, **27**, 344–351.
5. Sprinzl,M., Horn,C., Brown,M., Ioudovitch,A. and Steinberg,S. (1998) Compilation of tRNA sequences and sequences of tRNA genes. *Nucleic Acids Res.*, **26**, 148–153.
6. Hopper,A.K. and Phizicky,E.M. (2003) tRNA transfers to the limelight. *Genes Dev.*, **17**, 162–180.
7. Huh,W.K., Falvo,J.V., Gerke,L.C., Carroll,A.S., Howson,R.W., Weissman,J.S. and O'Shea,E.K. (2003) Global analysis of protein localization in budding yeast. *Nature*, **425**, 686–691.
8. Clark,T.A., Sugnet,C.W. and Ares,M., Jr (2002) Genomewide analysis of mRNA processing in yeast using splicing-specific microarrays. *Science*, **296**, 907–910.
9. Kuai,L., Fang,F., Butler,J.S. and Sherman,F. (2004) Polyadenylation of rRNA in *Saccharomyces cerevisiae*. *Proc. Natl Acad. Sci. USA*, **101**, 8581–8586.
10. Peng,W.T., Robinson,M.D., Mnaimneh,S., Krogan,N.J., Cagney,G., Morris,Q., Davierwala,A.P., Grigull,J., Yang,X., Zhang,W. *et al.* (2003) A panoramic view of yeast noncoding RNA processing. *Cell*, **113**, 919–933.
11. Hiley,S.L., Jackman,J., Babak,T., Trochesset,M., Morris,Q.D., Phizicky,E. and Hughes,T.R. (2005) Detection and discovery of RNA modifications using microarrays. *Nucleic Acids Res.*, **33**, e2.
12. Xing,F., Hiley,S.L., Hughes,T.R. and Phizicky,E.M. (2004) The specificities of four yeast dihydrouridine synthases for cytoplasmic tRNAs. *J. Biol. Chem.*, **279**, 17850–17860.
13. Giaever,G., Chu,A.M., Ni,L., Connelly,C., Riles,L., Veronneau,S., Dow,S., Lucau-Danila,A., Anderson,K., Andre,B. *et al.* (2002) Functional profiling of the *Saccharomyces cerevisiae* genome. *Nature*, **418**, 387–391.
14. Mnaimneh,S., Davierwala,A.P., Haynes,J., Moffat,J., Peng,W.T., Zhang,W., Yang,X., Pootoolal,J., Chua,G., Lopez,A. *et al.* (2004) Exploration of essential gene functions via titratable promoter alleles. *Cell*, **118**, 31–44.
15. Elela,S.A., Igel,H. and Ares,M., Jr (1996) RNase III cleaves eukaryotic preribosomal RNA at a U3 snoRNP-dependent site. *Cell*, **85**, 115–124.
16. Amberg,D.C., Goldstein,A.L. and Cole,C.N. (1992) Isolation and characterization of RAT1: an essential gene of *Saccharomyces cerevisiae* required for the efficient nucleocytoplasmic trafficking of mRNA. *Genes Dev.*, **6**, 1173–1189.
17. Hughes,T.R., Mao,M., Jones,A.R., Burchard,J., Marton,M.J., Shannon,K.W., Lefkowitz,S.M., Ziman,M., Schelter,J.M., Meyer,M.R. *et al.* (2001) Expression profiling using microarrays fabricated by an ink-jet oligonucleotide synthesizer. *Nat. Biotechnol.*, **19**, 342–347.
18. Chapman,K.B. and Boeke,J.D. (1991) Isolation and characterization of the gene encoding yeast debranching enzyme. *Cell*, **65**, 483–492.
19. Abelson,J., Trotta,C.R. and Li,H. (1998) tRNA splicing. *J. Biol. Chem.*, **273**, 12685–12688.
20. Ooi,S.L., Samarsky,D.A., Fournier,M.J. and Boeke,J.D. (1998) Intronic snoRNA biosynthesis in *Saccharomyces cerevisiae* depends on the lariat-debranching enzyme: intron length effects and activity of a precursor snoRNA. *RNA*, **4**, 1096–1110.
21. van Hoof,A., Lennertz,P. and Parker,R. (2000) Yeast exosome mutants accumulate 3′-extended polyadenylated forms of U4 small nuclear RNA and small nucleolar RNAs. *Mol. Cell. Biol.*, **20**, 441–452.
22. McCutcheon,J.P. and Eddy,S.R. (2003) Computational identification of non-coding RNAs in *Saccharomyces cerevisiae* by comparative genomics. *Nucleic Acids Res.*, **31**, 4119–4128.
23. Schattner,P., Decatur,W.A., Davis,C.A., Ares,M., Jr, Fournier,M.J. and Lowe,T.M. (2004) Genome-wide searching for pseudouridylation guide snoRNAs: analysis of the *Saccharomyces cerevisiae* genome. *Nucleic Acids Res.*, **32**, 4281–4296.
24. Mathews,D.H., Sabina,J., Zuker,M. and Turner,D.H. (1999) Expanded sequence dependence of thermodynamic parameters improves prediction of RNA secondary structure. *J. Mol. Biol.*, **288**, 911–940.
25. Zuker,M. (2003) Mfold web server for nucleic acid folding and hybridization prediction. *Nucleic Acids Res.*, **31**, 3406–3415.
26. Engelke,D.R., Gegenheimer,P. and Abelson,J. (1985) Nucleolytic processing of a tRNAArg-tRNAAsp dimeric precursor by a homologous component from *Saccharomyces cerevisiae*. *J. Biol. Chem.*, **260**, 1271–1279.
27. O'Connor,J.P. and Peebles,C.L. (1991) In vivo pre-tRNA processing in *Saccharomyces cerevisiae*. *Mol. Cell. Biol.*, **11**, 425–439.

28. Furter,R., Snaith,M., Gillespie,D.E. and Hall,B.D. (1992) Endonucleolytic cleavage of a long 3′-trailer sequence in a nuclear yeast suppressor tRNA. *Biochemistry*, **31**, 10817–10824.
29. Nagel,R. and Ares,M., Jr (2000) Substrate recognition by a eukaryotic RNase III: the double-stranded RNA-binding domain of Rnt1p selectively binds RNA containing a 5′-AGNN-3′ tetraloop. *RNA*, **6**, 1142–1156.
30. Chanfreau,G., Legrain,P. and Jacquier,A. (1998) Yeast RNase III as a key processing enzyme in small nucleolar RNAs metabolism. *J. Mol. Biol.*, **284**, 975–988.
31. O'Connor,J.P. and Peebles,C.L. (1992) PTA1, an essential gene of *Saccharomyces cerevisiae* affecting pre-tRNA processing. *Mol. Cell. Biol.*, **12**, 3843–3856.
32. Sharma,K., Fabre,E., Tekotte,H., Hurt,E.C. and Tollervey,D. (1996) Yeast nucleoporin mutants are defective in pre-tRNA splicing. *Mol. Cell. Biol.*, **16**, 294–301.
33. Shen,W.C., Selvakumar,D., Stanford,D.R. and Hopper,A.K. (1993) The *Saccharomyces cerevisiae* LOS1 gene involved in pre-tRNA splicing encodes a nuclear protein that behaves as a component of the nuclear matrix. *J. Biol. Chem.*, **268**, 19436–19444.
34. Thompson,M., Haeusler,R.A., Good,P.D. and Engelke,D.R. (2003) Nucleolar clustering of dispersed tRNA genes. *Science*, **302**, 1399–1401.
35. Bertrand,E., Houser-Scott,F., Kendall,A., Singer,R.H. and Engelke,D.R. (1998) Nucleolar localization of early tRNA processing. *Genes Dev.*, **12**, 2463–2468.
36. Grosshans,H., Hurt,E. and Simos,G. (2000) An aminoacylation-dependent nuclear tRNA export pathway in yeast. *Genes Dev.*, **14**, 830–840.
37. Sarkar,S. and Hopper,A.K. (1998) tRNA nuclear export in *Saccharomyces cerevisiae*: in situ hybridization analysis. *Mol. Biol. Cell*, **9**, 3041–3055.
38. Yoshihisa,T., Yunoki-Esaki,K., Ohshima,C., Tanaka,N. and Endo,T. (2003) Possibility of cytoplasmic pre-tRNA splicing: the yeast tRNA splicing endonuclease mainly localizes on the mitochondria. *Mol. Biol. Cell*, **14**, 3266–3279.
39. Schwer,B. and Shuman,S. (1996) Conditional inactivation of mRNA capping enzyme affects yeast pre-mRNA splicing *in vivo*. *RNA*, **2**, 574–583.
40. Eddy,S.R. (2002) Computational genomics of noncoding RNA genes. *Cell*, **109**, 137–140.
41. Wu,L.F., Hughes,T.R., Davierwala,A.P., Robinson,M.D., Stoughton,R. and Altschuler,S.J. (2002) Large-scale prediction of *Saccharomyces cerevisiae* gene function using overlapping transcriptional clusters. *Nature Genet.*, **31**, 255–265.
42. Paddison,P.J., Caudy,A.A., Bernstein,E., Hannon,G.J. and Conklin,D.S. (2002) Short hairpin RNAs (shRNAs) induce sequence-specific silencing in mammalian cells. *Genes Dev.*, **16**, 948–958.
43. Paddison,P.J., Caudy,A.A. and Hannon,G.J. (2002) Stable suppression of gene expression by RNAi in mammalian cells. *Proc. Natl Acad. Sci. USA*, **99**, 1443–1448.